JOURNAL OF PROPULSION AND POWER
Vol. 25, No. 2, March–April 2009

Jupiter Power Generation with Electrodynamic Tethers at Constant Orbital Energy

Claudio Bombardelli*
ESA, 2201 AZ Noordwijk, The Netherlands
Enrico C. Lorenzini†
University of Padova, 35131 Padova, Italy
and
Juan R. Sanmartin‡
Universidad Politécnica de Madrid, 28040 Madrid, Spain

DOI: 10.2514/1.38764

An electrodynamic tether system for power generation at Jupiter is presented that allows extracting energy from Jupiter's corotating plasmasphere while leaving the system orbital energy unaltered to first order. The spacecraft is placed in a polar orbit with the tether spinning in the orbital plane so that the resulting Lorentz force, neglecting Jupiter's magnetic dipole tilt, is orthogonal to the instantaneous velocity vector and orbital radius, hence affecting orbital inclination rather than orbital energy. In addition, the electrodynamic tether subsystem, which consists of two radial tether arms deployed from the main central spacecraft, is designed in such a way as to extract maximum power while keeping the resulting Lorentz torque constantly null. The power-generation performance of the system and the effect on the orbit inclination is evaluated analytically for different orbital conditions and verified numerically. Finally, a thruster-based inclination-compensation maneuver at apoapsis is added, resulting in an efficient scheme to extract energy from the plasmasphere of the planet with minimum propellant consumption and no inclination change. A tradeoff analysis is conducted showing that, depending on tether size and orbit characteristics, the system performance can be considerably higher than conventional power-generation methods.

Nomenclature

a	=	orbit semimajor axis
$\mathbf{B}$	=	magnetic field vector
B	=	magnetic field magnitude
B_S	=	Jupiter surface magnetic field magnitude at zero magnetic latitude (420 μT)
d	=	distance of the point of application of the Lorentz force from the cathodic end
$\mathbf{E}$	=	motional electric field
E_t	=	motional electric field projection along z
$\mathbf{E}_\pi$	=	the motional electric field projection on the tether rotation plane
e	=	orbit eccentricity
$\mathbf{F}$	=	rotation-averaged Lorentz force on a tether arm of length L
$\mathbf{F}_{\text{tot}}$	=	total Lorentz force on the spacecraft
$\mathbf{F}_1$	=	Lorentz force on the upper tether arm
$\mathbf{F}_2$	=	Lorentz force on the lower tether arm
H_0	=	reference height for the Divine–Garrett Jovian plasmasphere model
h	=	orbit angular momentum per unit mass
h_t	=	conductive-tape-tether thickness
I	=	tether current
I_C	=	tether current at the cathodic end
I_{av}	=	average current along the tether
$I_{\max}$	=	maximum current along the tether
I_0	=	reference current
i	=	orbit inclination
k	=	factor for generated power independent of electrodynamic tether location
k'	=	factor for Lorentz force independent of electrodynamic tether location
L	=	length of the tether arm
$\tilde{L}$	=	length of the bare portion of the tether arm
m_{SC}	=	spacecraft mass
m_T	=	total mass of the tethers
m_e	=	electron mass (9.1×10^{-31} kg)
N_e	=	plasmasphere electron density
N_0	=	reference density for the Divine–Garrett Jovian plasmasphere model (4.65×10^6 m^{-3})
q_e	=	electron charge (1.6×10^{-19} C)
R_J	=	Jupiter mean radius (71,492 km)
r_a	=	apoapsis radius
r_{SC}	=	spacecraft radial position along the orbit
r_0	=	reference radius for the Divine–Garrett Jovian plasmasphere model ($7.68R_J$)
$\mathbf{u}_E$	=	motional electric field unit vector
$\mathbf{u}_N$	=	Lorentz force unit vector
$\mathbf{u}_t$	=	tether-line unit vector
v_{exh}	=	propellant exhaust velocity
$\mathbf{v}_{\text{pl}}$	=	plasma velocity
$\mathbf{v}_{\text{sc}}$	=	spacecraft velocity
$\dot{W}$	=	power at the load
W_{EDT}	=	electric energy produced by the electrodynamic tether
W_{th}	=	propellant kinetic energy
w	=	conductive-tape-tether width
Z_C	=	impedance of load
$Z_{C,\text{opt}}$	=	power-optimum load impedance
z	=	tether-line abscissa
z^*	=	zero-bias abscissa
ΔV	=	spacecraft velocity increment for inclination-correction maneuver
Δm_f	=	ejected fuel mass for chemical thruster

Received 27 May 2008; revision received 3 November 2008; accepted for publication 4 December 2008.

*Research Fellow, Advanced Concepts Team.
†Professor, Department of Mechanical Engineering.
‡Professor, Department of Applied Physics, School of Aeronautical Engineering.

γ = ratio between tether-produced energy and propellant kinetic energy
δ = power density
ε = specific energy extracted from the planetary plasmasphere per unit variations of orbit inclination and spacecraft mass
ζ = nondimensional zero-bias abscissa
ζ_{opt} = power-optimum nondimensional zero-bias abscissa
ζ' = nondimensional zero-bias abscissa of the balancing tether arm
η = power-generation efficiency
μ = Jupiter gravitational constant
ν = true anomaly
ρ = density of tether material
σ = ratio between tether hardware mass and tether mass
τ = ratio of lower/upper tether arm Lorentz force
φ = angle between the tether line and the local motional electric field
Ω = Jupiter sidereal rotation rate ($\cong 1.77 \times 10^{-4}$ rad/s)
ω = argument of periapsis

I. Introduction

ALTHOUGH not yet part of conventional space hardware, electrodynamic tethers (EDTs) [1–3] are regarded as a very effective tool for future space exploration and utilization. This is especially true when we consider the recent advances in EDT mission design and, in particular, the development of the higher-efficiency bare-tether concept [4]. After the introduction of the latter, a substantial amount of research has been devoted to the understanding of the tether current-collection mechanism and the interaction with the surrounding magnetosphere [5–7]. In parallel to this activity, several applications of the bare EDT technology in space science and applications have been studied, ranging from propellantless propulsion to space power generation [8–10], including the use of EDTs as ionospheric science instruments [11].

An EDT can be used in generator mode (i.e., without an external power supply) for extracting useful power from the interaction with a planetary magnetosphere in the presence of plasma. In the general case, the power balance involves the orbital energy of the system, which is affected by the Lorentz force acting as drag (whereby the system loses orbital energy, resulting in orbit decay) or, in some circumstances, as thrust (whereby the system gains orbital energy, resulting in orbit raising). An example of a passive EDT system providing both thrust and power has been studied for the Jupiter system [10,12–14].

In some circumstances it may be desirable, due to specific mission constraints, to maintain the EDT in a constant-energy orbit while producing useful power. Although, in general, this will require correction maneuvers to be performed with an onboard propulsion system (hence at the expense of fuel mass), some exceptions exist. Peláez and Scheeres [15,16] have studied an EDT system that exploits the presence of the Jovian moonlets to eliminate the orbit drift while extracting power from the Jupiter environment. A similar scheme has been studied by Bombardelli et al. [17] to provide continuous power for an Io orbiter with a passive EDT.

Here, we investigate a means to produce power generation at constant orbital energy that exploits polar orbits. In this case, and assuming that the tether is lying in the orbit plane, the Lorentz force is directed orthogonally to the orbital plane and consequently affects the orbit inclination rather than the semimajor axis. As long as the inclination deviation remains small, the power extracted will come from the kinetic energy of the corotating plasma.

A promising application of this concept is to supply power for Jupiter exploration missions. Solar radiation at Jupiter is, on average, about 27 times less than on Earth, which implies the use of very large solar arrays or heavy and expensive radioisotope thermoelectric generators (RTGs), both solutions offering relatively low power density. On the other hand, high-throughput science missions require considerable power for both instruments and communications.

Previous work by Sanmartin and Lorenzini [10] and Sanmartin et al. [12–14] has shown that the Jupiter system is particularly suitable for operating EDT working in the generator mode because of its relatively strong magnetic field and fast-rotating plasmasphere. These same features make it particularly advantageous to extract energy from the plasmasphere with a polar-orbiting EDT. An additional advantage of polar orbits is that they provide a reduced radiation dose. For instance, the Juno mission [18], scheduled for launch in 2011, employs an 11-day elliptic polar orbit with periapsis at 1.06 Jupiter radii, which avoids the region of the trapped radiation belts, hence minimizing shielding requirements during the one-year nominal mission operation.

In this paper, we model the performance of a spinning bare EDT system around Jupiter considering polar orbits with generic eccentricity and argument of periapsis.

The reference spacecraft design consists of a central module spinning about an axis normal to the orbital plane and equipped with two bare EDTs of a few kilometers in length, deployed radially. The two tether arms operate as separate electrical systems, and as the spacecraft rotates, one arm provides power to the central part of the spacecraft, whereas the other is used to cancel out the overall Lorentz torque on the system. This mode of operation is convenient for an EDT in polar orbits, because the electrodynamic torque would otherwise induce an undesired precession of the spacecraft spin axis. Note that the price to pay is a reduction of the useful power that the overall tether length would otherwise provide. Although other methods proposed to control the average attitude of the tether axis have a smaller impact on the power-generation efficiency, the present scheme was chosen for its simplicity of implementation. For the case of gravity-gradient stabilized tethers, a method for eliminating Lorentz torques was proposed by Peláez and Sanjurjo [19].

The outline of the paper is the following. The power generation of a bare EDT and the optimal choice of the inserted load is investigated based on orbital motion limited (OML) plasma-collection theory [4]. Ohmic losses and ion collection are neglected, which is reasonable, considering the tether lengths to be used at Jupiter. Next, a self-balanced two-arm rotating EDT design is presented and analyzed. The fourth and fifth sections of the paper are devoted to the analytical computation of the rotation-averaged power along elliptical orbits and the variation of inclination due to the resulting Lorentz force. The effectiveness of an inclination-compensation maneuver is investigated in the sixth section. Finally, a numerical analysis is conducted to verify the validity of our simplifying assumptions, and a tradeoff analysis is conducted to compare the power density of the EDT with the one relative to RTGs and solar arrays.

II. Optimum Power Generation of an EDT with No Ohmic Effects

Let us consider a bare EDT (Fig. 1) of length L operating in the generator mode and flying along a generic orbit in the magnetosphere of a planet. The tether is a tape with a cross section of width w and thickness h_t (with $h_t \ll w$). Moreover, we assume that the tether maintains a rectilinear shape, where φ is the angle between the tether line and the local motional electric field $\mathbf{E}$ along the orbit, which is defined as

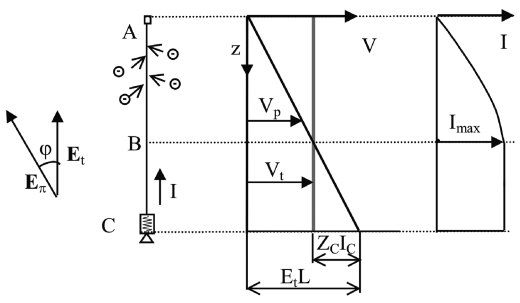

Fig. 1 Schematic of bare EDT working in generator mode with negligible ion collection on the negatively biased segment. *I* is the conventional (positive) current.

$$\mathbf{E} = \lfloor (\mathbf{v}_{sc} - \mathbf{v}_{pl}) \wedge \mathbf{B} \rfloor \tag{1}$$

where $\mathbf{B}$ is the local magnetic field, and $\mathbf{v}_{sc}$ and $\mathbf{v}_{pl}$ are the orbital velocity of the tether and the local velocity of the planet's corotating plasma.

A load of impedance Z_C is inserted in the circuit before the cathodic end for power-extraction purposes. Because of the relatively low density of Jupiter's magnetosphere, the current flowing into the EDT is small and ohmic effects can be neglected for tethers of practical size. Similarly, the ion current collection in the negatively biased portion of the tether can be neglected, as well as the losses at the anodic and cathodic ends of the tether.

Regarding the radiation impedance of various types of waves emitted by a tether carrying a steady current, they are known to be negligible in low Earth orbit. It has recently been shown, however, that the Alfven impedance, which is proportional to the Alfven velocity, can be greater at Jupiter by almost 3 orders of magnitude [20,21]; this will be considered in future work.

Under these assumptions and neglecting variations of magnetic field and plasma density along the tether length, the outside motional electric field can be assumed to be constant, as well as the potential inside the conductive tether. Hence, the potential difference between the tether surface and the plasma is linear with respect to the abscissa z from the anodic to the cathodic end (see Fig. 1) and it becomes null at a point z^*:

$$z^* = L - \frac{Z_C I_C}{E_t} \tag{2}$$

where E_t is the motional electric field projection along the tether line, and I_C is the current at the cathodic end.

The current gradient along the tether is as follows:

$$\frac{dI}{dz} > 0, \qquad z < z^* \tag{3a}$$

and

$$\frac{dI}{dz} = 0, \qquad z > z^* \tag{3b}$$

We will now compute the current profile assuming OML theory. This assumption is valid as long as the radius of a wire, or the equivalent radius $w/4$ in the case of a tape, is small compared with both the plasma Debye length λ_D and twice the electron gyroradius r_e [6]. In low Jovian orbit (periapsis down to $1.06R_J$), whereas λ_D is on the order of a meter, r_e can drop to about 3 cm. Ultimately, the following calculations are acceptable for an EDT not exceeding about 6 cm in width.

Then, under OML theory conditions and following the preceding simplifying assumptions, the current profile along the tether yields [4]

$$\frac{dI}{dz} = \frac{2w}{\pi} q_e N_e \sqrt{\frac{2q_e E_t (z^* - z)}{m_e}}, \qquad 0 < z < z^* \tag{4a}$$

$$\frac{dI}{dz} = 0, \qquad z^* < z < L \tag{4b}$$

where q_e is the electron charge magnitude of 1.6×10^{-19} C, m_e is the electron mass of 9.1×10^{-31} kg, and N_e is the plasma electron density.

The current profile is obtained after solving Eq. (4a) for $I(z = 0) = 0$ as

$$I(z) = \frac{4}{3}\frac{w}{\pi} q_e N_e \sqrt{\frac{2q_e E_t}{m_e}} [(z^*)^{3/2} - (z^* - z)^{3/2}] \quad 0 < z < z^* \tag{5}$$

After introducing the nondimensional zero-bias abscissa

$$\zeta = \frac{z^*}{L} = 1 - \frac{Z_C I_C}{E_t L} \tag{6}$$

the maximum current along the tether follows from Eqs. (5) and (6):

$$I_{max} = I_C = I_0 \zeta^{3/2} \tag{7}$$

where

$$I_0 = \frac{4}{3}\frac{w}{\pi} q_e N_e L^{3/2} \sqrt{\frac{2q_e E_t}{m_e}} \tag{8}$$

The average current along the tether can now be computed as

$$I_{av} = \frac{1}{L}\int_0^L I(z)\mathrm{d}z = \frac{(5 - 2\zeta)\zeta^{3/2}}{5} I_0 \tag{9}$$

Finally, the power at the load is

$$\dot{W} = Z_C I_C^2 = I_0 E_t L (1 - \zeta)\zeta^{3/2} \tag{10}$$

The value of ζ that provides maximum power generation is obtained by imposing a zero first derivative as

$$\zeta_{opt} = \tfrac{3}{5} \tag{11}$$

The corresponding load impedance is derived from Eqs. (6–8):

$$Z_{C,opt} = \frac{3\pi\sqrt{2}}{8} \cdot \frac{1 - \zeta_{opt}}{\zeta_{opt}^{3/2}} \sqrt{\frac{m_e}{q_e^3}} \frac{\sqrt{E_t}}{N_e w \sqrt{L}} \tag{12}$$

Equation (12) shows that the impedance needs to be continuously controlled to follow the variation of the motional electric field along the orbit. In addition, for the general case of rotating EDT, the impedance is modulated by the tether rotation.

The distance of the point of application of the Lorentz force from the cathodic end is

$$d = L - \frac{\int_0^L I(z) z \mathrm{d}z}{I_{av} L} = \frac{8\zeta^2 - 28\zeta + 35}{14(5 - 2\zeta)} L \tag{13}$$

which, for the power-optimized case, becomes

$$d(\zeta = 3/5) \cong 0.4L \tag{14}$$

III. Self-Balanced Two-Arm Rotating EDT

A scheme of the proposed rotating EDT system is depicted in Fig. 2. The current profile of the upper tether arm can be optimized to provide maximum power to the central module, as described previously. On the other hand, the current profile of the lower tether arm is tuned in such a way that the resulting Lorentz torque balances the torque on the upper arm. This can be done by insulating part of the tether closer to the central module and/or by tuning the impedance

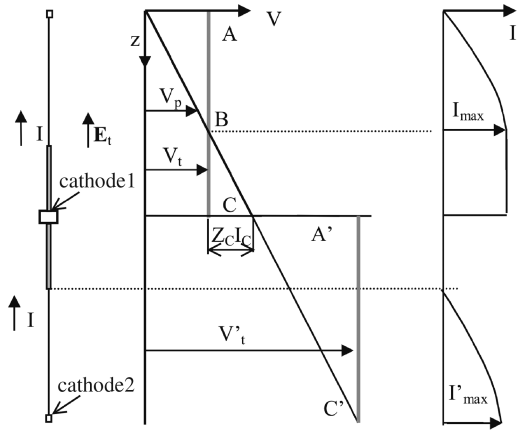

Fig. 2 Schematic of two-arm self-balanced rotating EDT working in generator mode. Both tether arms are insulated for about three-fifths of their length and no load is inserted in the lower arm. Two cathodes are active: one at the middle spacecraft and the other at the lower tether end.

inserted before the lower cathode. As ion collection is negligible, insulating a segment of the tether has virtually no effect on the current collection in the upper tether arm as long as the segment length is lower than the negatively biased portion of the tether. In contrast, the insulation in the lower tether arm reduces the electron collection and limits the resulting Lorentz force and torque.

Denoting $\tilde{L}$ as the length of the bare portion of each tether arm and denoting ζ' as the nondimensional zero-bias abscissa computed with respect to $\tilde{L}$ and the lower tether's impedance, the zero-torque condition can be written as

$$LI_{\mathrm{av}}(\zeta, L)d(L, \zeta) = \tilde{L}I_{\mathrm{av}}(\zeta', \tilde{L})[L - d(\tilde{L}, \zeta')] \tag{15}$$

Taking into account Eqs. (9), (13), and (15) yields

$$\frac{1}{14}L^{7/2}\zeta^{3/2}(8\zeta^2 - 28\zeta + 35) = \tilde{L}^{7/2}(5 - 2\zeta')\zeta'^{3/2}\left(\frac{L}{\tilde{L}} - \frac{8\zeta'^2 - 28\zeta' + 35}{14(5 - 2\zeta')}\right) \tag{16}$$

which can be solved numerically to provide $\zeta' = f(\zeta)$ once $\tilde{L}$ is set. In particular, it can be seen that for maximum power generation both at the middle point (main spacecraft) and at the lower tether end, the insulated length should be zero, and the condition for the load yields

$$\zeta'(\zeta = \tfrac{3}{5}) \cong 0.44 \tag{17}$$

On the other hand, a small insulated tether part may be required to avoid electrical breakdown between the two tether arms and the central part of the spacecraft. For the other extreme case in which the impedance in the lower tether is zero, the equilibrium condition yields the length of the bare part of the tether:

$$\tilde{L} \cong 0.62L \tag{18}$$

Note that for the optimum power-generation case, having about three-fifths of the tether length insulated has a negligible influence on the upper power-generating tether arm.

IV. Power Produced

Let us assume that the spin-stabilized EDT travels along an elliptic Keplerian orbit around Jupiter with 90 deg inclination, argument of pericenter ω, eccentricity e, semimajor axis a, and true anomaly ν and that the tether rotation plane coincides with the orbital plane (Fig. 3). The assumption of Keplerian orbit is justified by the fact that the most significant perturbations (namely, the acceleration associated with Jupiter's nonspherical potential and the Lorentz force) are expected to have a small impact on the power generation within the time scale of an orbit revolution. On a longer time scale, Jupiter's oblateness has an important secular effect causing a nonnegligible precession of the line of apses (for the Juno mission nominal orbit, [18] the precession is about -1 deg per orbit). To first order, the precession can be accounted for by updating the argument of periapsis after each orbit revolution. A numerical analysis that includes these effects is presented in Sec. VII.

In the following, we compute the motional electric field along the orbit assuming a nontilted zero-offset magnetic field model and the Divine–Garrett plasma density model [11]. The influence of a tilted magnetic field will be analyzed numerically in Sec. VII.

Given the preceding assumption and because the plasma velocity is always orthogonal to the orbital plane, the projection of the motional electric field on the tether rotation plane has the simple expression

$$\mathbf{E}_{\pi} = \mathbf{B} \wedge \mathbf{v}_{\mathrm{pl}} = Bv_{\mathrm{pl}}\mathbf{u}_E \tag{19}$$

where $\mathbf{B}$ is the magnetic field vector, $\mathbf{v}_{\mathrm{pl}}$ is the plasma velocity vector, and $\mathbf{u}_E$ is the motional electric field unit vector.

The magnitudes of the magnetic field and plasma velocity along the orbit are

$$B = \frac{B_S R_J^3}{r_{\mathrm{SC}}^3}\sqrt{1 + 3\sin^2(\omega + \nu)} \tag{20}$$

and

$$v_{\mathrm{pl}} = \Omega r_{\mathrm{SC}}|\cos(\omega + \nu)| \tag{21}$$

where R_J is the Jupiter's equatorial radius, $B_S \cong 420\ \mu$T is the planetary surface magnetic field magnitude at zero latitude, $\Omega \cong 1.77 \times 10^{-4}$ rad/s is Jupiter's sidereal rotation rate, and r_{SC} is the radial distance to the tethered system, which is given by

$$r_{\mathrm{SC}} = \frac{a(1 - e^2)}{1 + e\cos\nu} \tag{22}$$

After accounting for Eqs. (20–22), the magnitude of the motional electric field projected on the tether plane yields

$$E_{\pi} = \frac{\Omega B_S R_J^3|\cos(\omega + \nu)|(1 + e\cos\nu)^2\sqrt{1 + 3\sin^2(\omega + \nu)}}{a^2(1 - e^2)^2} \tag{23}$$

for which the component along the tether line is

$$E_t = E_{\pi}\cos\varphi \tag{24}$$

After plugging Eqs. (23) and (24) into Eq. (10) and assuming a constant ζ, the rotation-averaged power for a single tether arm of length L yields

$$\dot{W} = \frac{1}{\pi}\int_{-\pi/2}^{\pi/2}(\cos\varphi)^{3/2}\mathrm{d}\varphi \cdot \frac{4}{3}\frac{w}{\pi}q_e N_e E_{\pi}^{3/2}L^{5/2}\sqrt{\frac{2q_e}{m_e}}[(1 - \zeta)\zeta^{3/2}] = kwL^{5/2}N_e E_{\pi}^{3/2} \tag{25}$$

with

$$k = \frac{1}{\pi}\int_{-\pi/2}^{\pi/2}(\cos\varphi)^{3/2}\mathrm{d}\varphi \cdot \frac{4}{3\pi}\sqrt{\frac{2q_e^3}{m_e}}[(1 - \zeta)\zeta^{3/2}] = 0.334 \cdot \sqrt{\frac{q_e^3}{m_e}}[(1 - \zeta)\zeta^{3/2}] \tag{26}$$

For the case of highly eccentric orbits ($e > 0.9$) or low-altitude circular orbits ($a < 3.8R_J$), it is sufficient to consider the plasma electron density given by the Divine–Garrett model [22] for the inner plasmasphere of Jupiter ($R_J < r < 3.8R_J$). After neglecting longitude-related density variations, which mostly affect the lower-density high-latitude regions, we can write

$$N_e = N_0\exp\left[\frac{r_0}{r_{\mathrm{SC}}} - \left(\frac{r_{\mathrm{SC}}}{H_0} - 1\right)^2(\omega + \nu)^2\right] \tag{27}$$

where $r_0 = 7.68R_J$ (Jupiter radii) is the reference radius, $H_0 = R_J$ is the reference height, and $N_0 = 4.65 \times 10^6\ \mathrm{m}^{-3}$ is the reference density.

The final expression of the power generated along the orbit is derived from Eqs. (25–27) as

$$\dot{W}(\nu) = 0.334 \cdot N_0\exp\left[r_0\frac{1 + e\cos\nu}{a(1 - e^2)} - \left(\frac{a(1 - e^2)}{H_0(1 + e\cos\nu)} - 1\right)^2(\omega + \nu)^2\right] \cdot \left[\frac{\Omega B_s R_J^3|\cos(\omega + \nu)|(1 + e\cos\nu)^2\sqrt{1 + 3\sin^2(\omega + \nu)}}{a^2(1 - e^2)^2}\right]^{3/2} \times L^{5/2}w\sqrt{\frac{q_e^3}{m_e}}[(1 - \zeta)\zeta^{3/2}] \tag{28}$$

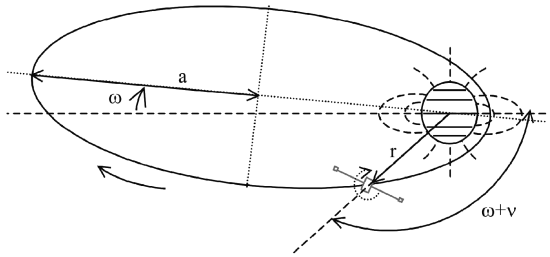

Fig. 3 Schematic of a polar orbit EDT around Jupiter as referred to in the current analytical model.

When intermediate orbits are considered, the expression of the plasma density is more involved, as different plasmasphere regions need to be considered simultaneously [20]. This generalization goes beyond the scope of the present paper.

Equation (28) is plotted in Figs. 4 and 5. Figure 4 shows the power generated in a Juno-type orbit [$e = 0.947$ and $r_p = 1.06R_J$ (see [18])] for different values of the tether arm length. Figure 5 shows the power generated in circular orbits of different radii. A considerably high level of power is produced even by relatively short tethers. Specifically, a 25 km tether can produce a peak power on the order of a megawatt.

V. Impact on Orbit Inclination

The rotation-averaged Lorentz force on a tether arm of length L is as follows:

$$\mathbf{F} = \frac{1}{\pi}\int_{-\pi/2}^{\pi/2}(LI_{\rm av}\mathbf{u}_t \wedge \mathbf{B})\mathrm{d}\varphi = \frac{1}{\pi}L\int_{-\pi/2}^{\pi/2}(I_{\rm av}\mathbf{u}_t)\mathrm{d}\varphi \wedge \mathbf{B} \tag{29}$$

where $\mathbf{u}_t$ is the tether-line unit vector. Because ζ is constant, we have

$$\int_{-\pi/2}^{\pi/2}(I_{\rm av}\mathbf{u}_t)\mathrm{d}\varphi = \int_{-\pi/2}^{\pi/2}\left(I_{\rm av}\frac{\mathbf{E}_\pi}{E_\pi}\right)\mathrm{d}\varphi = \int_{-\pi/2}^{\pi/2} I_{\rm av}\mathrm{d}\varphi\frac{\mathbf{E}_\pi}{E_\pi} \tag{30}$$

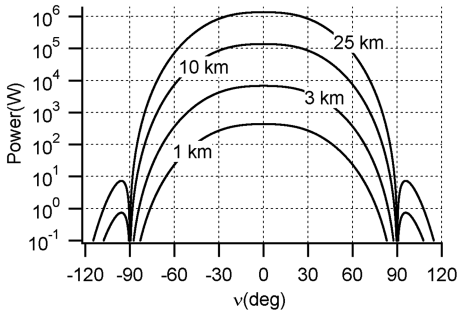

Fig. 4 Maximum power generated by a spinning bare EDT of different arm lengths in a polar elliptic orbit with $r_p = 1.06$ Jupiter radii and $e = 0.947$. Tether width is 5 cm.

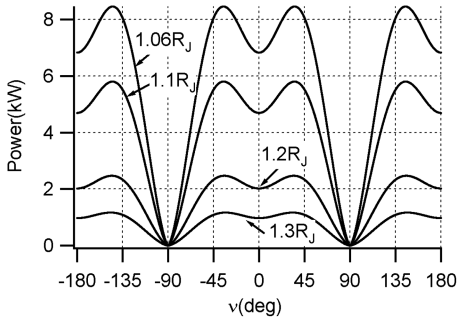

Fig. 5 Maximum power generated by a spinning bare EDT of 3 km arm length and 5 cm width in polar *circular* orbits of different radii. The data scale with tether length is $L^{5/2}$.

Taking into account Eqs. (30) and (9), Eq. (29) yields

$$\mathbf{F} = \frac{k' w L^{5/2} N_e}{\sqrt{E_\pi}}(\mathbf{E}_\pi \wedge \mathbf{B}) \tag{31}$$

where

$$k' = \frac{1}{\pi}\int_{-\pi/2}^{\pi/2}(\cos\varphi)^{3/2}\mathrm{d}\varphi \cdot \frac{4}{15\pi}\sqrt{\frac{2q_e^3}{m_e}}[(5-2\zeta)\zeta^{3/2}]$$
$$= 0.0667 \cdot [(5-2\zeta)\zeta^{3/2}]\sqrt{\frac{q_e^3}{m_e}} \tag{32}$$

Following Eq. (19) and applying the Lagrange triple-product formula, the force can be written in the compact form:

$$\mathbf{F} = \frac{k' w L^{5/2} N_e}{\sqrt{E_\pi}}[(\mathbf{B} \wedge \mathbf{v}_{\rm pl}) \wedge \mathbf{B}] = \frac{k' w L^{5/2} N_e}{\sqrt{E_\pi}} B^2 \mathbf{v}_{\rm pl}$$
$$= \frac{k' w L^{5/2} N_e E_\pi^{3/2}}{\Omega r_{\rm SC}\cos(\omega+\nu)}\mathbf{u}_n \tag{33}$$

When we consider a self-balanced rotating electrodynamic tether, the force exerted on the balancing tether arm has to be included such that the resulting force yields

$$\mathbf{F}_{\rm tot} = \mathbf{F}_1(L,\zeta) + \mathbf{F}_2(\tilde{L},\zeta') = (1+\tau)\mathbf{F}_1(L,\zeta) \tag{34}$$

with

$$\tau = \frac{F_2}{F_1} = \frac{\tilde{L}^{5/2}(5-2\zeta')\zeta'^{3/2}}{L^{5/2}(5-2\zeta)\zeta^{3/2}} \tag{35}$$

Specifically, for the power-optimized case ($\zeta = 3/5$) with fully bare tether arms ($\zeta' \cong 0.44$), $\tau = 0.68$. If the bare length of the tether is reduced to $0.62L$, we obtain $\tau = 0.51$.

The variation of the orbit inclination can now be computed using the Gauss equation:

$$\frac{di}{dt} = \frac{r_{\rm SC}\cos(\omega+\nu)}{h}\frac{F_{\rm tot}}{m_{\rm SC}} \tag{36}$$

where h is the orbit angular momentum per unit mass,

$$h = \sqrt{\mu a(1-e^2)} \tag{37}$$

and μ is the gravitational constant of Jupiter.

From Eqs. (33) and (34), Eq. (36) becomes

$$\frac{di}{dt} = \frac{k'(1+\tau) w L^{5/2} N_e E_\pi^{3/2}}{m_{\rm SC}\Omega h} \tag{38}$$

The derivative of the inclination with respect to the true anomaly can be computed from Eq. (38) after observing that

$$\frac{di}{d\nu} = \frac{di}{dt}\frac{dt}{d\nu} = \frac{di}{dt}\frac{r_{\rm SC}^2}{h} \tag{39}$$

which provides

$$\frac{di}{d\nu} = \frac{k'(1+\tau) r_{\rm SC}^2 N_e E_\pi^{3/2}}{m_{\rm SC}\Omega h^2} \tag{40}$$

After substituting Eqs. (23), (26), and (27) into Eq. (40) and integrating, we obtain the inclination variation per orbit revolution as

$$\Delta i_{\text{rev}} = \int_0^{2\pi} \left\{ 0.0667 \cdot N_0 \exp\left[r_0 \frac{1 + e\cos\nu}{a(1-e^2)} - \left(\frac{a(1-e^2)}{H_0(1+e\cos\nu)} - 1 \right)^2 (\omega+\nu)^2 \right] \cdot \frac{\sqrt{\Omega} B_s^{3/2} R_J^{9/2} |\cos(\omega+\nu)|^{3/2} (1+e\cos\nu)(1+3\sin^2(\omega+\nu))^{3/4}}{\mu m_{\text{SC}} a^2 (1-e^2)^2} \times L^{5/2} w \sqrt{\frac{q_e^3}{m_e}} \cdot (5-2\zeta)\xi^{3/2}(1+\tau) \right\} \mathrm{d}\nu \tag{41}$$

Results from Eq. (41) are plotted in Fig. 6 for a 1 t spacecraft with two 3-km-long tethers. The coefficient τ is set to 0.51 (partially insulated tethers). For EDT of generic length, the value of the inclination variation can be conservatively scaled with the $5/2$ power of the tether arm length as long as the impact of the tether mass on the overall spacecraft mass is neglected.

To determine the most suitable orbit design for power generation, it is useful to introduce the quantity

$$\varepsilon = \frac{1}{m_{\text{SC}}} \frac{dW}{di} \tag{42}$$

which corresponds to the *specific energy extracted from the rotating plasmasphere per unit variations of orbit inclination and spacecraft mass*.

From Eqs. (25), (38), (26), and (32), the quantity ε can be written in compact form as

$$\varepsilon = \frac{1}{m_{\text{SC}}} \frac{dW}{dt} \frac{dt}{di} = \frac{k}{k'} \frac{h\Omega}{1+\tau} = \eta h \Omega \tag{43}$$

where

$$\eta = \frac{5(1-\zeta)}{(5-2\zeta)(1+\tau)} \tag{44}$$

is the power-generation efficiency.

Notably, ε depends only on the orbit angular momentum, the plasma rotation rate, and the inserted load, whereas it is independent of tether geometry, characteristics of the magnetosphere, and the location along the orbit. Equation (43) shows that placing the tether in orbits with higher periapsis radii and eccentricities has a smaller effect on the inclination for the same energy extracted. On the other hand, we must stress that to reach the required power levels with reasonable tether lengths, the periapsis radius has to be kept sufficiently low.

For numerical cases, we consider the baseline Juno orbit ($e \cong 0.947$ and $r_p = 1.06R_J$) and a circular low-altitude orbit ($a = r_p = 1.3R_J$). In the first case, a spacecraft of 1000 kg equipped with two 3 km tethers can produce more than 1.3 kW average continuous power for a year, with less than 10 deg total inclination change. In the second case, the same spacecraft produces about 1 kW continuous power for a year, with the same inclination change.

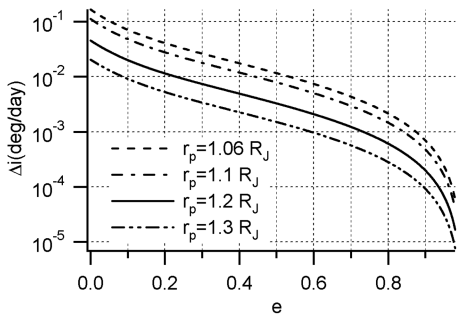

Fig. 6 Variation of inclination per day for a spinning self-balanced insulated EDT of 3 km arm length and a 1 t overall mass in a polar elliptical orbit with different eccentricities and periapsis distances. Tether width and thickness are 5 cm and 0.05 mm, respectively.

VI. Inclination Readjustment with Thrusters

Depending on power requirements and mission duration, it may be necessary to compensate for the variation in orbital inclination. For high-eccentricity orbits, this can be done very efficiently by thrusting at apoapsis to provide the required ΔV:

$$\Delta V = 2\sqrt{\frac{\mu(1-e)}{a(1+e)}} \sin\frac{\Delta i}{2} \tag{45}$$

As an example, for the nominal Juno orbit, only 27 m/s are required for every degree of inclination change.

It is interesting from the theoretical point of view to have a closer inspection at the energy balance. The kinetic energy provided by a chemical thruster can be written as

$$W_{\text{th}} = \tfrac{1}{2} \Delta m_f v_{\text{exh}}^2 \tag{46}$$

where Δm_f is the fuel mass ejected and v_{exh} is the (constant) propellant exhaust velocity. For chemical thrusters, the latter can reach about 3130 m/s employing a bipropellant engine.

For $\Delta m_f \ll m_{\text{SC}}$, we have

$$\Delta m_f \cong m_{\text{SC}} \frac{\Delta V}{v_{\text{exh}}} \tag{47}$$

so that the fuel kinetic energy required for the inclination change Δi results in

$$W_{\text{th}} \cong \frac{1}{2} m_{\text{SC}} v_{\text{exh}} \Delta V \cong \frac{1}{2} m_{\text{SC}} v_{\text{exh}} \sqrt{\frac{\mu(1-e)}{a(1+e)}} \Delta i \tag{48}$$

At the same time, the energy produced by the EDT over an orbit is

$$W_{\text{EDT}} = \int_0^T \dot{W} \mathrm{d}t = \int_0^T m_{\text{SC}} \varepsilon \frac{di}{dt} \mathrm{d}t = m_{\text{SC}} \varepsilon \Delta i \tag{49}$$

From Eqs. (48) and (49) and denoting r_a as the apoapsis radius, the ratio between energy produced and propellant kinetic energy yields

$$\gamma = \frac{W_{\text{EDT}}}{W_{\text{th}}} = \frac{2\varepsilon}{v_{\text{exh}}} \sqrt{\frac{a(1+e)}{\mu(1-e)}} = 2\eta \frac{\Omega r_a}{v_{\text{exh}}} \tag{50}$$

Remarkably, for a Juno-type orbit [18] with a power-optimized tether ($\zeta = 3/5$) and employing a bipropellant engine, γ reaches a value of 103. Consequently, the specific kinetic energy of the propellant is boosted from 1.36 to 140 kWh/kg, reaching more than 7 times the typical energy density of RTGs over a one-year mission.

VII. Numerical Analysis

To check the validity of the primary simplifying assumptions done so far, numerical simulations were conducted with a full model, including a tilted-dipole magnetic field, a complete gravitational model [23], and the effect of the Lorentz force on the orbit evolution. The tether spin axis was assumed to retain an inertially fixed orientation.

The first test case was performed considering a circular orbit with a radius of $1.06R_J$. Results from the comparison are plotted in Fig. 7. The power generated appears to be mostly influenced by the 9.6 deg tilted dipole of Jupiter that, due to its 2.4 rev/day precession, modulates the useful power, causing considerable fluctuations. The J_2 component of Jupiter gravitational field has a much smaller influence, although it is not negligible. In spite of the fluctuations mentioned previously, the average value of the useful power is seen to vary by less than 5% from the analytical value. As for the inclination variation, the numerical results show good agreement with the analytical results, as long as the inclination change is less than, say, 2 deg. Note that due to Jupiter's magnetic dipole tilt, and as the orbit inclination departs from 90 deg, a small component of the Lorentz force parallel to the orbital velocity appears, which tends to slowly deorbit the tether. For example, a semimajor axis variation of

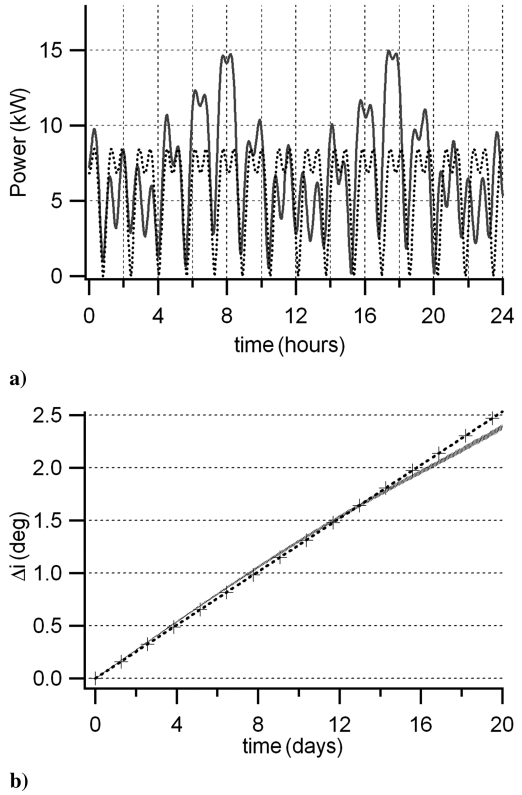

Fig. 7 Comparison between results of a fully numerical model (gray) and our simplified analytical model (dotted dark) for a) generated power and b) inclination variation for a circular polar orbit of radius $r = 1.06R_J$ using two 3-km-long, 5-cm-thick, self-balanced electrodynamic tethers.

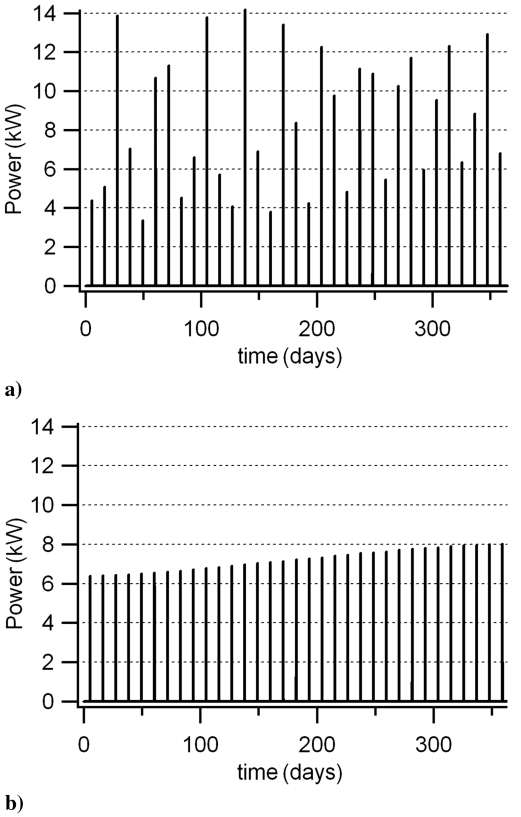

Fig. 8 Comparison between results of a) a fully numerical model and b) our simplified analytical model for the power generated along an elliptic Juno-like polar orbit ($r = 1.06R_J$ and $e = 0.947$) using two 3-km-long, self-balanced electrodynamic tethers.

less than 0.4% was observed after a month for the 1 t spacecraft equipped with two 3 km tethers. A detailed investigation of these effects will be conducted in the future.

Similar considerations apply to the case of elliptical orbits. The analytical–numerical comparison for the power generation along a Juno-like orbit is shown in Fig. 8.

VIII. Tradeoff with Other Power-Generation Methods

The performance of the EDT as a power-generation system is compared here with more conventional power-generation methods that have been used or proposed for Jupiter missions: namely, RTGs and solar panels.

Because the performance of an EDT depends on the specific spacecraft location and relative velocity with respect to the ambient plasma, the power density is a function of the true anomaly. This is in contrast with RTGs, which have virtually constant power density throughout the whole mission. For solar arrays, the power density can also be considered to be constant, provided that there are no eclipses and that sun tracking is enabled. These issues make a direct comparison not straightforward.

When the mission involves circular or low-eccentricity orbits, the EDT is able to provide power most of the time, and one can use the peak power density and the average power density computed along the whole orbit as tradeoff metrics.

The peak EDT power density can be computed as

$$\delta(\nu) = \left(\frac{\dot{W}}{m_T + m_H}\right)_{\max} \tag{51}$$

where m_T is the overall tether mass (two arms) and m_H is the tether-related hardware mass (e.g., hollow cathods, deployers, etc.). The latter can be considered to be proportional to the former through a coefficient σ. Suggested values are $\sigma = 2$–2.5 [9], and the expression of the generated power is given by Eq. (25). In this way, Eq. (51) yields

$$\delta_{\max} = \frac{kL^{3/2}}{2\rho h_t(1+\sigma)} \max(N_e E_\pi^{3/2} | \nu = 0, \ldots, 2\pi) \tag{52}$$

where ρ is the tape-tether material density and h_t is its thickness. We will refer to aluminum tapes of $h_t = 0.05$ mm. An aluminum conductive tape tether of such thickness has been recently manufactured by the University of Tokyo for an upcoming suborbital EDT experiment [24]. Similarly, the average power density over the whole orbit yields

$$\delta_{\text{av}} = \frac{kL^{3/2}}{4\pi\rho h_t(1+\sigma)} \int_0^{2\pi} N_e E_\pi^{3/2} \mathrm{d}\nu \tag{53}$$

An additional complexity is encountered when high-eccentricity orbits are considered. As seen in the previous sections, in this case, the EDT will be able to provide power only in the proximity of Jupiter, while leaving most of the orbit "power-starved." Clearly, for a mission for which the power-demanding operations are distributed along the whole orbit, it is not convenient to use an EDT as the *only* power-generation system, because it would imply storing a large share of the energy in heavy storage devices. The EDT could yet be employed *in conjunction* with solar arrays or RTGs to provide high power levels around periapsis when needed (e.g., for data relay).

However, for missions using high-eccentricity orbits for which the main power-demanding operations are concentrated around the periapsis region, as the Juno mission, the EDT can still represent a valid alternative to conventional systems. In this case, we can introduce another tradeoff metric (namely, the average power computed along a 180 deg arc across periapsis):

$$\delta_{\text{per}} = \frac{kL^{3/2}}{2\pi\rho h_t(1+\sigma)} \int_0^{\pi} N_e E_\pi^{3/2} \mathrm{d}\nu \tag{54}$$

Table 1 Jupiter power density comparison between EDT and conventional systems

Type of orbit	RTGs	Solar arrays	Short EDT ($L_{tot} = 6$ km)	Long EDT ($L_{tot} = 50$ km)
Circular orbit $a = 1.06r_J$	1–8 W/kg	5–20 W/kg	70 W/kg (peak) 49 W/kg (average)	1579 W/kg (peak) 969 W/kg (average)
Circular orbit $a = 1.3r_J$	1–8 W/kg	5–20 W/kg	9.6 W/kg (peak) 6.7 W/kg (peak)	229.4 W/kg (peak) 157.4 W/kg (average)
Juno orbit $r_p = 1.06r_J$ $e = 0.947$	1–8 W/kg	5–20 W/kg	56.16 W/kg (peak) 14.5 W/kg (average)[a]	1348 W/kg (peak) 348 W/kg (average)[a]

[a]Average is computed along a 180 deg orbit arc around periapsis.

Based on Eqs. (52–54), a numerical comparison has been conducted and the results are summarized in Table 1. The coefficient σ has been set to a value of 2.

IX. Conclusions

A power-generation scheme involving self-balanced bare EDT in polar orbits around Jupiter has been presented. Simple analytical formulas were derived that allow the evaluation of the average power produced along a polar elliptical orbit and the effect on the orbit inclination.

Results show that using modestly sized tethers (two tethers of 3 km length), peak power of the level of a few kilowatts can be obtained for periapsis distances of less than 1.3 Jupiter radii (below Jupiter radiation belts). As the power generated scales with the $5/2$ power of the tether length, megawatt power levels can be obtained by just using 25-km-long tethers. The corresponding power density can reach peak levels of more than 1000 W/kg.

As far as the inclination variation is concerned, the large angular momentum of Jupiter orbits makes it possible to extract a considerable amount of power while keeping the orbit close to polar. For instance, an average power of 1 kW bears the cost of less than a 10 deg inclination variation per year in the worst-case scenario.

Finally, the design proposed in this paper can be exploited for converting the power associated with chemical thrusters into electrical power by performing an inclination-correction maneuver at apoapsis. For high-eccentricity orbits, the energy obtained can be a hundred times more than the kinetic energy of the thrusters, proving that the largest part of the energy produced is indeed extracted from the rotating plasmasphere.

The validity of the analytical formulation presented was checked with a more complex numerical model, showing that Jupiter's magnetic axis tilt has an important effect on the instantaneous power generated and a weak effect on orbital energy, whereas the orbital inclination and the average power produced do not change appreciably.

Acknowledgments

We would like to thank the Associate Editor and the reviewers for the useful comments and the promptness of the review process.

References

[1] Drell, S., Foley, H. M., and Ruderman, M. A., "Drag and Propulsion of Large Satellites in the Ionosphere: An Alfven Propulsion Engine in Space," *Journal of Geophysical Research*, Vol. 70, No. 13, 1965, pp. 3131–3145. doi:10.1029/JZ070i013p03131

[2] Grossi, M. D., "Spaceborne Long Vertical Wire as Self-Powered ULF/ELF Radiator," *IEEE Journal of Oceanic Engineering*, Vol. 9, No. 3, 1984, pp. 211–213. doi:10.1109/JOE.1984.1145613

[3] Dobrowolny, M., "Electrodynamics of Long Metallic Tethers in the Ionospheric Plasma," *Radio Science*, Vol. 13, No. 3, 1978, pp. 417–424. doi:10.1029/RS013i003p00417

[4] Sanmartin, J. R., Martinez-Sanchez, M., and Ahedo, E., "Bare Wire Anodes for Electrodynamic Tethers," *Journal of Propulsion and Power*, Vol. 9, No. 3, May–June 1993, pp. 353–360. doi:10.2514/3.23629

[5] Sanmartin, J. R., and Estes, R. D., "Magnetic Self-Field Effects on Current Collection by an Ionospheric Bare Tether," *Journal of Geophysical Research*, Vol. 107, No. A11, 2002, p. 1335. doi:10.1029/2002JA009344

[6] Sanmartin, J. R., and Estes, R. D., "The Orbital Motion Limited Regime of Cylindrical Langmuir Probes," *Physics of Plasmas*, Vol. 6, No. 1, 1999, pp. 395–405. doi:10.1063/1.873293

[7] Khazanov, G. V., Stone, N. H., Krivorutsky, E. N., Gamauynov, K. V., and Liemohn, M. W., "Current-Induced Magnetic Field Effects on Bare Tether Current Collection: A Parametric Study," *Journal of Geophysical Research*, Vol. 106, No. 10, 2001, p. 565.

[8] Estes, R. D., Lorenzini, E. C., Sanmartin, J., Peláez, J., Martinez-Sanchez, M., and Johnson, C. L., "Bare Tethers for Electrodynamic Spacecraft Propulsion," *Journal of Spacecraft and Rockets*, Vol. 37, No. 2, 2000, pp. 205–211. doi:10.2514/2.3567

[9] Ahedo, E., and Sanmartin, J. R., "Analysis of Bare-Tether Systems for Deorbiting Low-Earth-Orbit Satellites," *Journal of Spacecraft and Rockets*, Vol. 39, No. 2, Mar.–Apr. 2002, pp. 198–205. doi:10.2514/2.3820

[10] Sanmartin, J. R., and Lorenzini, E. C., "Exploration of Outer Planets Using Tethers for Power and Propulsion," *Journal of Propulsion and Power*, Vol. 21, No. 3, May–June 2005, pp. 573–576. doi:10.2514/1.10772

[11] Sanmartin, J. R., Charro, M., Peláez, J., Tinao, I., Elaskar, S., Hilgers, A., and Martinez Sanchez, M., "Floating Bare Tether as Upper Atmosphere Probe," *Journal of Geophysical Research*, Vol. 111, Nov. 2006, Paper A11310.

[12] Sanmartin, J. R., Charro, M., Lorenzini, E. C., Garrett, H. B., Bombardelli, C., and Bramanti, C., "Electrodynamic Tether at Jupiter, 1: Capture Operations and Constraints," *IEEE Transactions on Plasma Science*, Vol. 36, No. 5, Oct. 2008, pp. 2450–2458. doi:10.1109/TPS.2008.2002580

[13] Sanmartin, J. R., Charro, M., Lorenzini, E. C., Garrett, H. B., Bombardelli, C., and Bramanti, C., "Electrodynamic Tether at Jupiter, 2: Fast Moon Tour After Capture," *IEEE Transactions on Plasma Science* (to be published).

[14] Sanmartin, J. R., Charro, M., Lorenzini, E., and Garrett, H., "Electrodynamic Tether Microsats at the Giant Planets," ESA, Advanced Concepts Team, Rept. 05-3203, Noordwijk, The Netherlands, 2006.

[15] Peláez, J., and Scheeres, D. J., "A Permanent Tethered Observatory at Jupiter: Dynamical Analysis," *Advances in the Astronautical Sciences*, Vol. 127, 2007, pp. 1307–1330.

[16] Peláez, J., and Scheeres, D. J., "On the Control of a Permanent Tethered Observatory at Jupiter," 2007 AAS/AIAA Astrodynamics Specialist Conference, Mackinac Island, MI, American Astronautical Society Paper AAS07-369, Aug. 2007.

[17] Bombardelli, C., Lorenzini, E. C., Curreli, D., Sanjurjo-Rivo, M., Lucas, F., Peláez, J., and Lara, M., "Io Exploration with Electrodynamic Tethers," *2008 AIAA/AAS Astrodynamics Specialist Conference* (to be published).

[18] Matousek, S., "The Juno New Frontiers Mission," *Acta Astronautica*, Vol. 61, No. 10, Nov. 2007, pp. 932–939. doi:10.1016/j.actaastro.2006.12.013

[19] Peláez, J., and Sanjurjo, M., "Generator Regime of Self-Balanced Electrodynamic Bare Tethers," *Journal of Spacecraft and Rockets*, Vol. 43, No. 6, Nov.–Dec. 2006, pp. 1359–1369. doi:10.2514/1.20471

[20] Charro, M., and Sanmartin, J. R., "Waves Radiated by an Electrodynamic Tether over the Jovian Polar Caps," *2007 AGU Fall Meeting*, American Geophysical Union Abstract P53A-1005, Dec. 2007.

[21] Torres, A. S., Sanmartin, J. R., and Donoso, J. M., "The Radiation

Impedance of an Electrodynamic Tether in Jovian Polar Orbit," *COSPAR 08* (to be published).

[22] Divine, N., and Garrett, H. B., "Charged Particle Distribution in Jupiter's Magnetosphere," *Journal of Geophysical Research*, Vol. 88, No. A9, Sept. 1983, pp. 6889–6903. doi:10.1029/JA088iA09p06889

[23] Campbell, J. K., and Synott, S. P., "Gravity Field of the Jovian System from Pioneer and Voyager Tracking Data," *Astronomical Journal*, Vol. 90, Feb. 1985, pp. 364–372. doi:10.1086/113741

[24] Fujii, H. A., Takegahara, H., Oyama, K., Sasaki, S., Yamagiwa, Y., Kruijff, M., Vander Heide, E. J., Sanmartin, J. R., and Charro, M., "A Proposed Bare-Tether Experiment on Board a Sounding Rocket," 2nd International Energy Conversion Engineering Conference, Providence, RI, AIAA, Paper 2004-5718, Aug. 2004.

G. Spanjers
Associate Editor